ELSEVIER

Journal of Fluorine Chemistry 114 (2002) 163–170

JOURNAL OF FLUORINE CHEMISTRY

www.elsevier.com/locate/jfluchem

Enhanced Lewis acidity by aliovalent cation doping in metal fluorides

E. Kemnitz[a,*], Y. Zhu[b], B. Adamczyk[a]

[a]*Institute of Chemistry, Humboldt University Berlin, Hessische Str. 1-2, D-10115 Berlin, Germany*
[b]*Institute of Physical Chemistry, Peking University, 100871 Bejing, PR China*

Received 18 September 2001; accepted 9 January 2002

Abstract

A model regarding the generation of acidity in binary metal fluorides has been proposed and its validity has been examined for several binary fluoride systems with the general compositions $MF_3/M'F_3$ and $MF_2/M'F_3$. In accordance with this hypothesis, the binary systems (CrF_3/AlF_3, CrF_3/FeF_3 and AlF_3/VF_3) do not show acidities larger than the sum of the acidities of the component fluorides. The hypothesis predicts the generation of Lewis acidity when MF_2 is the major component (host) and generation of Brønsted acidity when MF_3 acts as the host for the $MF_2/M'F_3$. The experimental results (surface acidity and catalytic activity) confirmed the predictions made from this hypothesis for binary combinations $MgF_2/M'F_3$ (M' = Cr, Al, Fe, V). The application of this model is discussed in terms of other parameters: ionic radii and the fluoride affinity of the metal fluorides involved.

1. Introduction

Lewis acids are commonly used as catalysts in fluorination reactions. Among very strong Lewis acids like SbF_5 or $Sb(F,Cl)_5$ [1], which are used mainly in homogeneous reactions, solid metal fluorides, especially AlF_3 and CrF_3 are attractive Lewis acid catalysts for gas phase fluorination reactions ([2] and references therein). Recently, aluminum chlorofluoride (ACF) has been found as a strong solid Lewis acid which, as evidenced for several fluorination reactions under identical conditions, is a stronger acid than SbF_5 [3,4]. Unfortunately, the compound's extremely hygroscopic nature limits its easy application for technical reactions and nothing is known about the structure of this catalyst. Based on theoretical fluoride affinity calculations at the correlated MP2/PDZ level theory [5], a pF scale has been established which shows that aluminum fluoride as well as ACFs could be considered as strong as the strongest known Lewis acid (SbF_5). However, this might be true for molecular structures of these compounds which is not the case for AlF_3. Hence, AlF_3 evidently exhibits weaker Lewis acidity and thus, the catalytic activity is lower than that found for SbF_5 and ACF [3]. Moreover, the existence of several meta-stable AlF_3 phases is known in addition to the thermodynamically stable α-AlF_3, which differ significantly in their catalytic activity. All these structures are build up by corner shared AlF_6 octahedra. The α-phase has a close-packed structure [6], whereas, β-AlF_3 has a more open structure of the hexagonal tungsten bronze (HTB) type [7]. The other phases that have been characterized structurally are related to β-AlF_3 [8]. Although α-AlF_3 has little or no catalytic activity, the β-phase is an active heterogeneous catalyst for the dismutation of chlorofluoromethanes and hydrochlorofluoromethanes [9,10]. The β-, η-, θ- and κ-phases are active catalysts for the fluorination of $CHCl_3$ or CCl_3CF_3 by anhydrous hydrogen fluoride [11]. It has been suggested, therefore, that the former materials have a surface structure that resembles that of β-AlF_3 with coordinatively unsaturated surface Al^{3+} sites [9]. Although this is undoubtedly a simplification, the available evidence indicates that Lewis surface sites are present in the meta-stable AlF_3 phases what is not the case in the close-packed α-AlF_3. The discrepancy between the calculated and the experimentally determined Lewis acidity of AlF_3 and $Al(Cl,F)_3$ phases reflects the absence of suitable synthesis procedures for potential solid Lewis acids. Evidently, the Lewis acidity of metal(III) fluorides, especially in case of AlX_3 phases, strongly depends on the bulk structure: In crystalline close-packed structures of metal fluorides, the M^{3+} cations are coordinatively saturated by the fluoride anions and thus, can not act as Lewis sites. Consequently, the search for alternative synthesis routes for meta-stable or strongly distorted metal fluorides is a challenging task. An

* Corresponding author. Tel.: +49-30-2093-7555;
fax: +49-30-2093-7277.
E-mail address: erhard.kemnitz@chemie.hu-berlin.de (E. Kemnitz).

0022-1139/02/$ – see front matter
PII: S0022-1139(02)00022-2

alternative option for generating Lewis acidity in metal fluorides is doping with other metals. Unfortunately, less systematic work has been done so far, therefore, results of doping in metal fluorides and their impact on the catalytic activity is limited.

Numerous procedures have been developed to generate Brønsted or Lewis acidity in metal oxide hosts. To best of our knowledge, nothing comparable is known for metal fluorides up until now. An attractive model to predict whether Lewis or Brønsted acidity can be generated in a host lattice by introducing of an additional metal has been developed by Tanabe [13]. This model predicts which binary oxides will show acidic properties (Brønsted or Lewis) and provides insight regarding the structure of the acid sites.

We report the results of adapting the Tanabe model [13] to binary metal fluorides here and show how Brønsted or Lewis acidity, respectively, can be predicted by choosing the right metal fluoride combination.

2. Results and discussion

2.1. The model

By applying the Tanabe model on binary metal fluoride systems, acidity generation is caused by an excess of a positive or negative charge in the model structure of a binary fluoride. This structural model is based on the following assumptions.

(i) The coordination number of a positive element of a metal fluoride (MF_n) and that of a second metal fluoride ($M'F_m$) are maintained even when mixed.
(ii) The coordination number of a negative element (fluoride) of a major component fluoride is retained for all the fluorides in a binary fluoride.

For example, the model structure of the solid solution of CrF_3/MgF_2, where CrF_3 is the major component fluoride, and that of MgF_2/CrF_3, where MgF_2 is the major component fluoride, are shown in Fig. 1a and b, respectively. The coordination numbers of the cations in the component single fluorides remain 6 for both Cr and Mg, when they are mixed, whereas, those of the fluoride anions should be 2 and 3, respectively, according to the postulates (i) and (ii). In the case of Fig. 1a, the two positive charges of the magnesium atom are distributed over six bonds, i.e. +2/6 positive charge for each bond, while the negative charge of the fluoride atom is distributed over two bonds with −1/2 of a valence unit for each bond. The difference in charge for one bond is $+(2/6)-(1/2)=-1/6$ and the valence unit of $-(1/6)\times 6=-1$ is excess for all bonds. In this case, Brønsted acidity is expected because one proton is assumed (originated from moisture or, if present, HF) to associate with the fluoride ions to keep electrical neutrality.

In the case of Fig. 1b, the positive charge of +3 for the chromium atom is also distributed to six bonds, i.e., +3/6 positive charges for six bonds. Since the fluoride ions in this structure are three-fold, just −1/3 of a valance unit is found in each bond. The difference in charge for one bond is $+3/6-(1/3)=+1/6$ and the valence unit of $+(1/6)\times 6=+1$ is excess for all bonds. Here, Lewis acidity is expected due to the generation of an excess of positive charge.

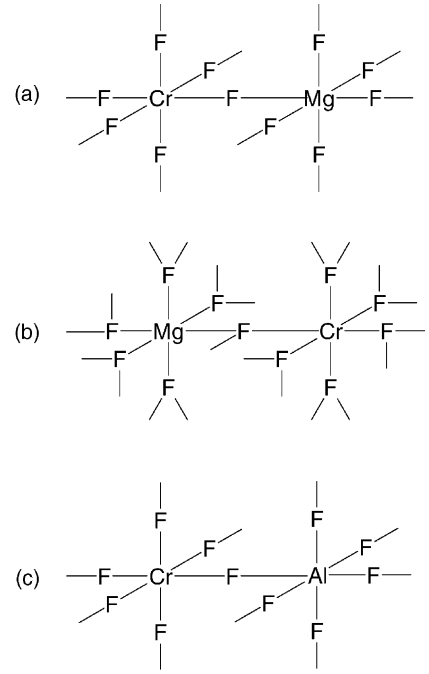

Fig. 1. Model structure of a binary metal fluoride system pictured according to postulates (i) and (ii) for: (a) CrF_3/MgF_2 when CrF_3 is the major fluoride; (b) MgF_2/CrF_3 when MgF_2 is the major fluoride; (c) CrF_3/AlF_3 when CrF_3 is the major fluoride.

If we consider a system of isotypic MF_3 phases, which are very commonly used as industrial fluorination catalysts, the situation seems different. For a system like AlF_3/CrF_3, there is no excess charge available according to our model structure resulting from postulates (i) and (ii), as illustrated by Fig. 1c. Therefore, this binary system is not expected to show any additional acidic properties. As will be shown later, this agrees with our experimental results.

The validity of this hypothesis was examined for several combinations of the binary metal fluorides: (i) $MF_3/M'F_3$ and (ii) $MgF_2/M'F_3$ (Table 1).

As probe reactions for the catalytic activity of these binary fluoride catalysts the following fluorination reactions were employed:

$$\text{dismutation of } CCl_2F_2: \quad 2CCl_2F_2 \rightarrow CCl_3F + CClF_3 \quad (1)$$

$$\text{hydrofluorination of } C_2Cl_4: \quad CCl_2CCl_2 + (x+1)HF \rightarrow C_2HCl_{4-x}F_{x+1} + xHCl \quad (2)$$

For the heterogeneously catalyzed fluorination reactions (1) and (2), Lewis acid surface sites are required. This is obvious already due to the fact that both reactions start immediately

Table 1
Characteristic bulk and surface properties and catalytic behavior of selected pure and binary metal fluorides

Sample	Optimal composition M/(M + M′)	X-ray powder crystallinity	S_{BET} (m^2/g)	Conversion in dismutation reaction[a]	Acid sites (FT-IR photoacoustic)	
					Lewis	Brønsted
Pure phases						
α-AlF_3	–	α-AlF_3 (good)		–	–	–
β-AlF_3	–	β-AlF_3 (good)	31	×	×	–
α-CrF_3	–	α-CrF_3 (partial amorphous)	74	×	×	–
β-CrF_3	–	β-CrF_3 (good)	38	×	×	–
$Cr(F,OH)_3$	$CrF_{0.41}(OH)_{2.59}$	Pyrochlore (amorphous)	10	–	–	Traces
α-FeF_3	–	α-FeF_3 (good)	8	–	–	–
β-FeF_3	Maximum temperature 300 °C	β-FeF_3 (good)	24	×	×	–
β-VF_3	–	β-VF_3	18	×	×	–
MgF_2	–	MgF_2 (good)	10	–	Traces	–
Modified phases						
AlF_3/Cr	AlF_3/Cr8	β-AlF_3 (good)	54	×	×	–
CrF_3/Al	$Cr(OH,F)_3$/Al20	Amorphous	100	×	×	Traces
FeF_3/Cr	FeF_3/Cr35	β-FeF_3 (low)	39	×	×	–
CrF_3/Fe	$Cr(OH,F)_3$/Fe23	Pyrochlore (low)	13	×	×	Traces
AlF_3/V	AlF_3/V14	β-AlF_3 (less crystalline)	13	×	×	–
VF_3/Al	VF_3/Al33	β-VF_3, α-VF_3, α-AlF_3	15	×	×	–
MgF_2/Cr	MgF_2/Cr8	MgF_2 (partial amorphous)	78	×	×	–
CrF_3/Mg	$Cr(OH,F)_3$/Mg26	Pyrochlore (amorphous)	15	Traces	Traces	Traces
MgF_2/Al	MgF_2/Al50	MgF_2 + β-AlF_3	45	–	β-AlF_3	–
AlF_3/Mg	AlF_3/Mg20	β-AlF_3 + MgF_2	42	Traces	×	–
MgF_2/Fe	MgF_2/Fe15	MgF_2 (partial amorphous)	35	×	×	–
FeF_3/Mg	FeF_3/Mg20	MgF_2 (partial amorphous)	22	–	Traces	Traces
MgF_2/V	MgF_2/V15	MgF_2 (low)	116	×	×	–

[a] Probe reaction for the catalytic behavior. Dismutation of CCl_2F_2: $2CCl_2F_2 \rightarrow CCl_3F + CClF_3$.

when pure MF_3 phases which are known to be suitable Lewis acid catalysts are employed. However, due to the presence of HF in the reaction (2), the formation of a Lewis site/HF complex ($M^{3+} \cdots F{-}H$) is very probable which may result in the formation of an intermediate "Brønsted surface complex" at the surface during the reaction. Nevertheless, the reaction starts at a surface Lewis site and therefore, has to be considered as a Lewis catalyzed reaction.

As stated above, β-MF_3 phases occurring in the HTB structure have been proven to be better solid Lewis acids and hence, are more active catalysts for heterogeneous fluorination reactions than the thermodynamic stable α-modifications ([12] and references therein). Consequently, the synthesis conditions for our investigations were chosen to obtain preferentially the β-MF_3 phases, this was not possible in all cases.

The MgF_2/MF_3 systems differ in detail but their properties obtained as a result of the doping follow a general rule. Therefore, the characteristic results obtained for the MgF_2/VF_3 system that has not been described in the literature by now, will be described in detail. This is followed by a comparison of the main results for all the other systems.

2.2. The MF_3/$M'F_3$ system

The detailed results of the investigations for the binary systems β-(Al/Cr)F_3 [14] and β-(Cr/Fe)F_3 [15] have already been described in the literature. Here, we summarize the main properties of these systems that are relevant for discussion. The main properties of the β-(Al/V)F_3 system which has not been published until now will also be considered in this context.

For all three systems, X-ray phase analysis indicates a partial incorporation of the minor component because the host MF_3 phase is the only crystalline phase detectable. In the case of the AlF_3/CrF_3 system, the crystallinity decreases with increasing Cr^{3+} content and results in a nearly complete amorphous phase at a Cr content of about 80% which still shows very weak peaks of β-AlF_3 [14]. Under these synthesis conditions, the pure CrF_3 system in fact consists of $Cr(F,OH)_3$ having the pyrochlore structure. The catalytic activity of these samples is very similar; only a slight increase was observed for Cr concentrations between 10 and 50%, which is accompanied by a drastic increase of the BET surface area. Pure $Cr(F,OH)_3$ is not catalytically active. Thus, this binary metal fluoride system does not show acidity larger than the sum of the acidity of the component fluorides consistent with the Tanabe model. The observed slight increase of activity might simply be due to the increased BET surface area of the samples as a result of the decreasing X-ray crystallinity. A similar observation was made in case of the CrF_3/FeF_3 system [15]. However, more distinctly than for the (Al/Cr)F_3 system, a sharp change of the structure type formed was found depending on the guest/host metal ratio, i.e. at a Fe/Cr atomic ratio above 50%, the only detectable crystalline phase was β-FeF_3, whereas, the

only detectable crystalline phase below this value (excess of Cr) was the pyrochlore $Cr(F,OH)_3$. Here too, the catalytic activity increased from 10 to 35% Cr, which was accompanied by an increase of the BET surface even in this system.

The formation of solid solutions occurring in the β-AlF_3 structure was observed as expected on the basis of the similar anionic radii of Al^{3+} and V^{3+}. Even for this system, we observed a catalytic activity and acidity which might be explained in terms of the sum of the acidities of the component fluorides.

All the $(M/M')F_3$ phases investigated form solid solutions with significantly larger BET surface areas when the ionic radii do not differ by more than 15%. According to the Tanabe model, no generation of additional acidity should be expected for this system. However, a slight increase of the concentration of surface acid sites and also slightly increased catalytic activity was observed probably due to the increased surface area (more disturbed surface).

2.3. The MgF_2/MF_3 systems

The MgF_2/MF_3 systems listed in Table 1 differ in detail but their general properties obtained as a result of doping follow a general rule. Since the systems MgF_2/AlF_3 and MgF_2/CrF_3 have already been described in detail [14,15], we concentrate on the new systems MgF_2/VF_3 and MgF_2/FeF_3 with special emphasis on the MgF_2/VF_3 binary system here. Based on this, the other systems will be discussed in a more generalized context.

2.4. MgF_2/VF_3

2.4.1. X-ray diffraction and BET analysis

The surface areas for selected samples of this system vary significantly with the dopant concentration (Table 2). Interestingly enough, the main pore diameter is significantly larger (300–500 Å) for the pure metal fluorides, although that of VF_3 covers a wide range, whereas, that of the binary systems are in the range of only 40–80 Å (Fig. 2). By analogy with the respective AlF_3 system, the thermal decomposition of α-$VF_3 \cdot 3H_2O$ results in the formation of crystalline β-VF_3 which is iso-structural to β-AlF_3 (curve "e" in Fig. 3). This phase is stable up to 723 K.

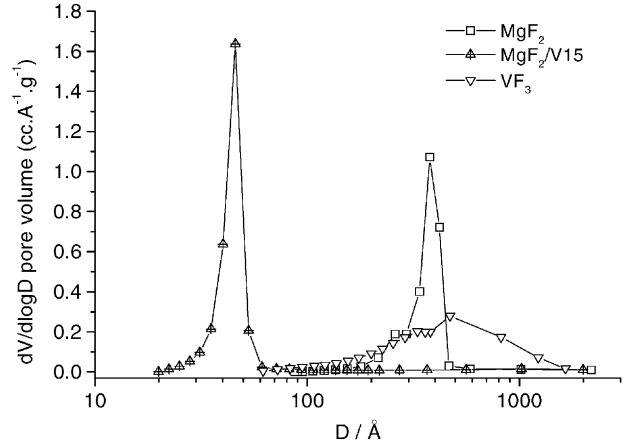

Fig. 2. Pore size distribution for selected MgF_2/VF_3 samples.

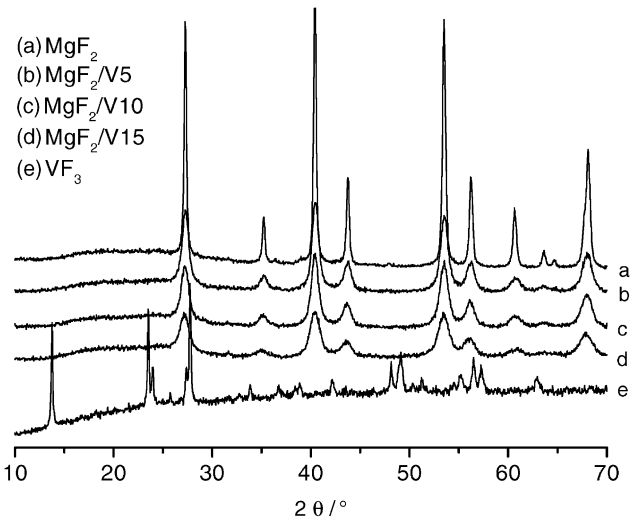

Fig. 3. XRD patterns of MgF_2/VF_3 samples.

MgF_2 calcined at 693 K shows good crystallinity (curve "a" in Fig. 3). The similarity in the ionic radii of Mg^{2+} (0.72 Å) and V^{3+} (0.64 Å) [16], provides for the formation of solid solution in this system which is confirmed by the XRD patterns, although these phases are less crystalline as compared with the pure fluorides. As shown in Fig. 3, there

Table 2
Characteristic data for MgF_2/VF_3 binary system

Sample-composition	X-ray powder analysis	Crystallinity	S_{BET} (m^2/g)	Conversion (%)[a]	Acid sites (FT-IR photoacoustic)	
					Lewis	Brønsted
MgF_2	MgF_2	Good	10	–	–	–
MgF_2/V5	MgF_2	Good/decreasing	68	55	×	–
MgF_2/V10	MgF_2	Medium	71	52	×	–
MgF_2/V15	MgF_2	Medium	116	89	×	–
β-VF_3	β-VF_3 (HTB)	Good	18	18	×	–

[a] Probe reaction for the catalytic activity. Hydrofluorination of TCE: $CCl_2CCl_2 + (4+x)HF \rightarrow C_2HCl_{(4-x)}F_{(x+1)}$ (number in brackets indicates percentage conversion at 553 K).

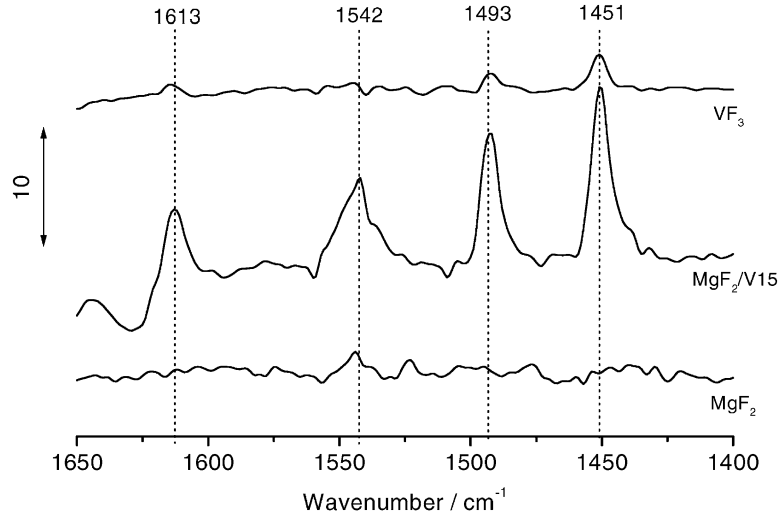

Fig. 4. FT-IR photoacoustic spectra of pyridine chemisorbed on MgF_2/VF_3 samples (background correction, 80 mg catalyst weight, 30 ml pyridine adsorption at 523 K, flow system).

is no detectable shift of the reflections with increasing V^{3+} concentration. Instead, the appropriate doping causes a decrease in the crystallinity of the host lattice (MgF_2).

2.4.2. Surface acidity

Fig. 4 shows the normalized FT-IR photoacoustic spectra of pyridine that was chemisorbed on the solid surfaces. Lewis acidity is not detectable in pure MgF_2, it increases significantly with the V content and reaches a maximum for samples with about 85% Mg and 15%V (the band at 1451 cm^{-1} is characteristic for Lewis sites [10]). As expected, pure β-VF_3 also posseses surface Lewis sites. A maximum number of Lewis sites is observed for samples that have the maximum in BET surface area (Table 2). As found already for other systems [14,15], the maximum acidity and catalytic activity was found in the range between 5 and 20% of V^{3+}. In this system too, the optimum composition was found to be of around 15% V^{3+} in MgF_2 (Mg85) as shown in

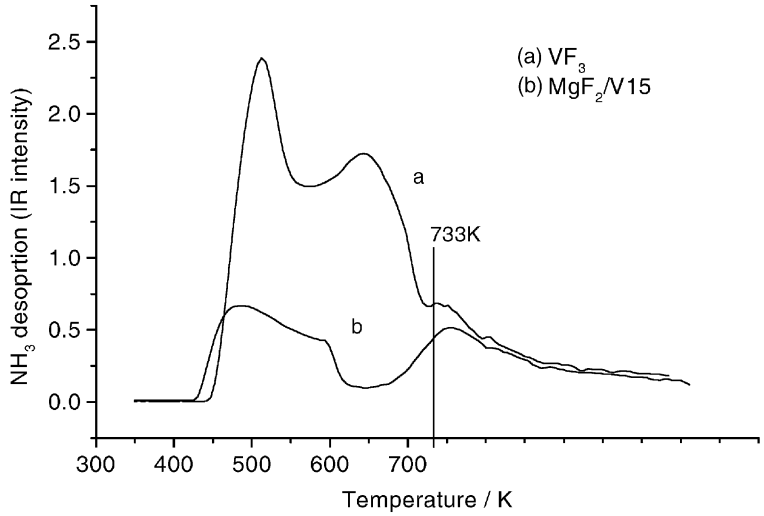

Fig. 5. The NH_3-TPD profiles for MgF_2/VF_3 samples.

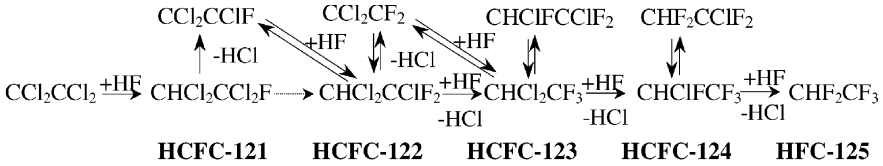

Scheme 1. Reaction path of the catalyzed fluorination of TCE with HF.

Fig. 4. Comparing the temperature-programmed desorption of ammonia (NH_3-TPD) spectra for pure VF_3 and MgF_2/V15, provides further information (Fig. 5). The overall acidity in the case of VF_3 is significantly larger but this sample exhibits lower catalytic activity. This seems contradictory at first, but may be understood in that the TPD spectra give the sum of Lewis and Brønsted acidity and do not distinguish between them. However, more important is probably the fact that the sample MgF_2/V15 exhibits a relatively larger region of strong Lewis acid sites (those at higher temperatures).

2.4.3. Catalytic activity

The Lewis acid catalyzed fluorination of tetrachloroethylene (TCE) with HF as summarized in Scheme 1 was used to characterize catalytically these samples. As can be concluded from the product distribution (Fig. 6), the reaction consists obviously of a complex system of consecutive and competitive side reactions making the exact analytical investigation complicated. However, based on the experimental data, a simplified reaction pathway may be provided, as is summarized in Scheme 1.

Fig. 6 presents results for the catalyzed fluorination of C_2Cl_4 with gaseous HF and the product distribution as a function of the V content. The differences correspond to the number of Lewis acid sites derived from Fig. 4. Consistent with the expectation, almost no conversion was achieved using MgF_2 as catalyst. Little conversion could be observed only at temperatures as high as 733 K.

The situation described above is exactly paralleled in the MgF_2/CrF_3 system which has been described in detail in [15]. The MgF_2/FeF_3 system also follows this role although the increase of acidity and catalytic activity is mainly determined by the "weaker" Fe^{3+} compared to Al^{3+}, Cr^{3+} or V^{3+}, respectively. As can be seen in Table 1, the system MgF_2/AlF_3 did not form solid solutions because the anionic radii differ too much. Consequently, the observed acidic and catalytic properties of these samples reflect the sum of the catalytically active β-AlF_3 (minor component) and the catalytically inactive MgF_2 (major component) and hence, are not reliable in this context.

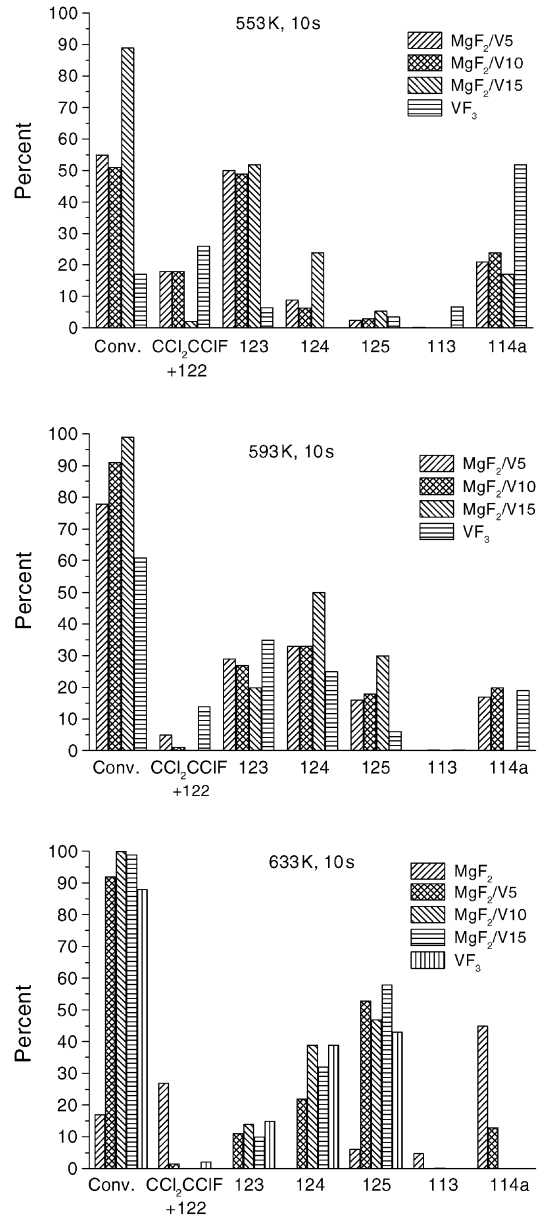

Fig. 6. Conversion of C_2Cl_4 and product distribution vs. V content for various MgF_2/VF_3 samples and different temperatures (catalyst mass 300 mg, residence time 1 s).

Table 3
Characteristic data for the binary system MgF_2/FeF_3

Sample composition	X-ray powder analysis	Crystallinity	S_{BET} (m^2/g)	Conversion (%)[a]	Acid sites (FT-IR photoacoustic)	
					Lewis	Brønsted
MgF_2	MgF_2	Good	10	–	–	–
MgF_2/Fe7	MgF_2	Partial amorphous	17	25	×	–
MgF_2/Fe15	MgF_2	Partial amorphous	35	50	×	–
MgF_2/Fe30	MgF_2	Partial amorphous	41	48	×	–
MgF_2/Fe80	MgF_2	Partial amorphous	31	17	×	Traces
FeF_3	β-FeF_3	Less crystalline	17	13	×	–

[a] Probe reaction for the catalytic activity. Hydrofluorination of TCE: $CCl_2CCl_2 + (4+x)HF \rightarrow C_2HCl_{(4-x)}F_{(x+1)}$ (number in brackets indicates percentage conversion at 633 K).

2.4.4. MgF_2/FeF_3

The characteristic data of this system are summarized in Table 3. The pure fluorides MgF_2 and even FeF_3 are catalytically inactive under the reaction conditions employed, whereas, the binary solid solutions show remarkably good catalytic activity. It must be born in mind, that FeF_3 is present as α-FeF_3 under these synthesis conditions (final calcination step for all samples, the pure and the binary fluorides, at 673 K) which, therefore, exhibits just low catalytic activity as was found for α-AlF_3 [14] too. As in the case of all the other systems (especially MgF_2/VF_3), the optimal composition for high catalytic activity is in the range between 15 and 30% FeF_3 in the MgF_2 host lattice and drops with further increase of the FeF_3 content. Interestingly enough, doping MgF_2 with FeF_3 resulted in phases which consist of X-ray crystalline MgF_2 and a second X-ray amorphous phase even at high Fe loading. That means, under these synthesis conditions, the catalytic active Fe/MgF_2 phase appears highly amorphous; this does, however, not invalidate the Tanabe model.

3. Conclusions

Although only a limited number of examples are available [14,15], the model described, once developed for binary metal oxides, might also be applicable to binary metal fluorides. Thus, a prediction of whether Brønsted or Lewis acidity will be generated as a result of doping a host by a suitable guest metal fluoride seems possible. In agreement with these predictions, solid solutions of different metal(III) fluorides (the most industrially applied fluorination catalysts) do not result in a synergistic effect regarding the observed acidity. Even the addition of metal(II) fluorides to MF_3 hosts does not result in any advantageous catalytic activity. In line with the prediction from the model, the formation of Brønsted sites was found, e.g. the formation of pyrochlore $M(F,OH)_3$ phases in case of doping a MF_3 host with a MF_2 guest (cf. the systems MF_3/MgF_2 with M = Al, Cr, Fe; Table 1). Contrary to the latter case, doping a MF_2 host by a metal(III) fluoride results in high surface area and very active binary metal fluoride phases as predicted from our model. Thus, all MF_2/MF_3 systems follow a general rule by forming a solid solution of the MF_2 host phase with a broad compositional range of amorphous phases. The catalytically most active phases are just in the compositional range with highly amorphous phases. Consequently, it is hard to decide whether the catalytic behavior observed follows strictly the prediction according the Tanabe model or it is just the effect of enhanced surface area accompanied by a significantly higher degree of distortion and thus, better availability of Lewis surface sites. However, even in the $MF_3/M'F_3$ systems, the formation of amorphous phases was observed, but without any significant positive effect on the catalytic activity of these samples which is an argument for the validity of the Tanabe model. Moreover, the MF_2/MF_3 solid solutions exactly followed the prediction from the model. Therefore, the Tanabe model seems applicable to metal fluorides.

Since the Tanabe model can predict only whether or not Lewis or Brønsted acidity might be generated in a binary metal fluoride system, it is not possible to draw conclusions about the strength of the acid sites generated. However, based on the pF scale established by Christe et al. [5], the most interesting elements might be selected for the system compositions.

A substantial pre-condition for the applicability of this model is the formation of solid solutions between the respective metal fluorides. This clearly is limited by the compatibility of the size of the cationic radii of the metals, as evidenced for the MgF_2/AlF_3 system. The formation of a solid solution can only be expected when the ionic radii fit together (S.D. $\pm$15%). Hence, the number of possible metal fluoride combinations is strongly restricted.

4. Experimental

4.1. Preparation of binary metal fluorides

4.1.1. MgF_2/FeF_3 and FeF_3/CrF_3

Appropriate amounts of the metal nitrates (typically in the range between 3 and 5 g) were dissolved in ethanol (50 ml) to make a mixture solution. The ethanol solution was then added dropwise to a 30 ml HF solution (40%) under stirring. After stirring for 0.5 h, the precipitate was filtered and washed with a small amount of de-ionized water/ethanol, then dried at room temperature and calcined at 693 K (2 K/min from room temperature to 693 K) for 2 h in N_2 under a self-generated atmosphere [7].

4.1.2. MgF_2/VF_3

V_2O_3 was dissolved in 40% HF (solution A) and magnesium nitrate was dissolved in ethanol (solution B). Solution B was then added to solution A quickly under rigorous stirring. After further stirring for 0.5 h, the precipitate was filtered and washed with small a amount of de-ionized water and ethanol, then dried and calcined under similar condition as described above. The washing process to remove the ethanol from the precipitate should preferably be performed under nitrogen atmosphere in order to prevent any oxidation of V^{III}.

The syntheses of all other binary metal fluoride systems discussed here are found in [14,15].

4.2. Catalyst characterization

X-ray powder diffraction characterization was carried on a XRD 7 Seiffert-FPM with Cu Kα radiation.

FT-IR photoacoustic pyridine adsorption spectroscopy was carried out according to the following procedure. A sample (80 mg) was pre-treated at 423 K under a nitrogen

flow of 35 ml/min for 15 min, then 60 μl pyridine was injected to the sample tube. The sample was flushed with nitrogen for another 15 min to remove physisorbed pyridine. Spectra of the sample was recorded at room temperature using a MTEC cell and FT-IR system 2000 (Perkin-Elmer). Spectra of the samples without pyridine absorption was also measured as the background.

The NH_3-TPD was employed for the determination of the strength distribution in the acid sites. The sample (200 mg, 0.3–0.5 mm diameter fraction) was pre-treated under nitrogen (35 ml/min) at 673 K for 1 h, then cooled to 393 K and exposed to NH_3. The physisorbed ammonia was removed over 1 h at 393 K. After cooling down to 353 K, the TPD program (10 K/min, up to 733 K, keeping 30 min) was started. The desorption of ammonia was monitored by continuous running IR spectroscopy (FT-IR system 2000, Perkin-Elmer).

The characteristic data for related samples are summarized in Table 1.

4.3. Catalysis

Catalytic testing was carried out using a flow reactor (nickel tube). The sample (0.5–0.8 mm particles) was first pre-treated in situ at 573 K under N_2 for 0.5 h and then fluorinated at 673 K in a gas mixture of 7.0 ml/min HF and 6.3 ml/min N_2 for 2 h. The catalytic reaction was investigated using a source gas of 1.2 ml/min C_2Cl_4 + 7.0 ml/min HF + 6.3 ml/min N_2, a contact time of 10 s was used for the regular test at different temperatures. The product was analyzed by GC–FID with a 10% SE 30 Chromosorb column. GC–MS was also used for the identification of the byproducts.

References

[1] C.G. Krespan, V.A. Petrov, Chem. Rev. 96 (1996) 3269.
[2] E. Kemnitz, D.-H. Menz, Prog. Solid State Chem. 26 (1998) 87.
[3] A.C. Sievert, C.G. Krespan, F.J. Weigert, US Patent 5,157,171 (1992), to DuPont.
[4] V.A. Petrov, C.G. Krespan, B.E. Smart, J. Fluorine Chem. 77 (1996) 139;
V.A. Petrov, C.G. Krespan, B.E. Smart, J. Fluorine Chem. 89 (1998) 125.
[5] K.O. Christe, D.A. Dixon, D. Mc Lemore, W.W. Wilson, J.A. Sheehy, J.A. Boatz, J. Fluorine Chem. 101 (2000) 151.
[6] R. Hoppe, D. Kissel, J. Fluorine Chem. 24 (1984) 327.
[7] A. Le Bail, C. Jacoboni, M. Leblanc, R. De Pape, H. Duroy, J.L. Fourquet, J. Solid State Chem. 77 (1988) 96.
[8] U. Bentrup, Eur. J. Solid State Inorg. Chem. 29 (1992) 51;
N. Herron, D.L. Thorn, R.L. Harlow, F. Davidson, J. Am. Chem. Soc. 115 (1993) 3028;
N. Herron, R.L. Harlow, D.L. Thorn, Inorg. Chem. 32 (1993) 2985;
N. Herron, D.L. Thorn, R.L. Harlow, G.A. Jones, J.B. Parise, J.A. Fernandez-Baca, T. Vogt, Chem. Mater. 7 (1995) 75;
C. Alonso, A. Morato, F. Medina, F. Guirado, Y. Cesteros, P. Salagre, J.E. Sueiras, R. Terrado, A. Giralt, Chem. Mater. 12 (2000) 1148.
[9] A. Hess, E. Kemnitz, A. Lippitz, W.E.S. Unger, D.-H. Menz, J. Catal. 148 (1994) 270.
[10] A. Hess, E. Kemnitz, J. Catal. 149 (1994) 449.
[11] N. Herron, W.E. Farneth, Adv. Mater. 8 (1996) 959.
[12] E. Kemnitz, J.M. Winfield, in: T. Nakajima, B. Žemva, A. Tressaud (Eds.), Advanced Inorganic Fluorides, Elsevier, Lausanne, 2000, pp. 367–401 (Chapter 12).
[13] K. Tanabe, Bull. Chem. Soc. Japan 47 (1974) 1064.
[14] E. Kemnitz, A. Hess, G. Rother, S.I. Troyanov, J. Catal. 159 (1996) 332.
[15] A. Adamczyk, A. Hess, E. Kemnitz, J. Mater. Chem. 6 (1996) 1731.
[16] R.D. Shannon, Acta Crystallogr. A32 (1976) 751.